Renewable Energy 238 (2025) 121914

Contents lists available at ScienceDirect

Renewable Energy

journal homepage: www.elsevier.com/locate/renene

Life cycle cost analysis of circular photovoltaic façade in dense urban environment using 3D modeling

Qingxiang Li [a,b], Lingege Long [c,d,*], Xinwei Li [b], Guidong Yang [a], Chenhang Bian [e], Benyun Zhao [a], Xi Chen [a,**], Ben M. Chen [a]

[a] Department of Mechanical and Automation Engineering, The Chinese University of Hong Kong, Shatin, NT, Hong Kong
[b] Architecture, Built Environment and Construction Engineering Department, Politecnico di Milano, Milan, 20100, Italy
[c] School of Art and Design, Beijing Institute of Fashion Technology, Beijing, 100029, China
[d] Department of Architecture and Urban Studies, Politecnico di Milano, Milan, 20100, Italy
[e] School of Science and Technology, Hong Kong Metropolitan University, Hong Kong

ARTICLE INFO

Keywords:
Photovoltaic façade
Circular economy
Perovskite solar cell
Recycling strategy
Distributed energy

ABSTRACT

Photovoltaic façade gradually diffuses in dense urban environment for decarbonization. In this study, life cycle cost analysis is applied to assess the economic feasibility of circular photovoltaic façade. An innovative aerial video-based 3D modeling method is developed to reconstruct the target structures, significantly reducing time and labor costs in modeling work. Given the recycling potential, this study develops a workflow to recycle photovoltaic components to save the spence. Multi-objective optimization is conducted to identify the optimal configuration of photovoltaic facades given an initial budget constraint. A representative building in Central Business District is selected to validate the effectiveness of the proposed method. Then the simulation is extended to major metropolises in China. The results demonstrate that the 3D modeling method can successfully reconstruct target structures, allowing for accurate simulation of solar radiation access and assessment of the economic feasibility of photovoltaic facades. Moreover, the photovoltaic façade on the selected building is not profitable without recycling. Some cities achieve profitability when the proposed recycling strategy is implemented. This highlights the importance of recycling in achieving economic viability. The study promotes further studies exploring the feasible deployment of photovoltaic façades in dense urban environments.

1. Introduction

Building sector plays an important role in achieving sustainable development goals (SDGs) outlined by the United Nations [1], especially in dense urban environment. The emission of the building sector accounts for more than one-third of the total emission, which is critical for achieving the ambitious decarbonization target. Practitioners widely acknowledge solar energy use as a potential way to reduce energy demand of buildings. Integrating photovoltaics on the building envelope, termed Building Integrated Photovoltaics (BIPV), attracts more attention to realize carbon neutrality in dense urban environment [2].

Traditional silicon PV technology has been mature for many years. However, it is rare to see the BIPV projects in high-density cities [3]. The primary reason is that the output of traditional PV panels is significantly influenced by the shadow created by surrounding buildings [4]. On the partial shadow condition, due to the nonlinear output characteristics of silicon PV panels, the power output will be significantly decreased [5]. Therefore, the silicon PV modules can be only applied on the building roof, but not the vertical facade despite its far larger area [6]. Moreover, the majority of building projects encounter challenges with rigid and heavy flat PV modules, as they contribute to increased envelope loads. Integration of PV modules demands robust structures capable of supporting their weight, often necessitating reinforcement of substructures like curtain walls. Consequently, such adaptations escalate installation costs [7]. The application of BIPV in urban areas is hindered by the dense urban planning and the prevalence of high-rise buildings.

1.1. Circular perovskite solar cell façade

The development of perovskite solar cells (PSCs) creates hope for the

* Corresponding author. School of Art and Design, Beijing Institute of Fashion Technology, Beijing, 100029, China.
** Corresponding author.
E-mail addresses: lingege.long@bift.edu.cn (L. Long), xichen002@cuhk.edu.hk (X. Chen).

https://doi.org/10.1016/j.renene.2024.121914
Received 1 August 2024; Received in revised form 9 November 2024; Accepted 14 November 2024
Available online 16 November 2024
0960-1481/

BIPV diffusion in the high-density urban environment. The world's first 1 GW perovskite photovoltaic production line has begun investment and construction in Wuxi, China [8]. PSC is regarded as an ideal material to be the next generation of solar cells for vertical BIPV systems [9]. The power conversion efficiency (PCE) of PSC has increased significantly during the past ten years, reaching over 25 %. Additionally, PSC panels can be directly adhered to the building envelope without requiring additional substructures, and can thus be integrated easily as light-weight construction [10]. Furthermore, PSC panels' ability to regulate color is another advantage in building applications for satisfying architects' aesthetics concerns. They also outperform silicon solar cells in low light and diffuse light conditions when applied on vertical envelopes in dense cities.

However, PSCs has a relatively short lifespan, less than 2 years, requiring frequent replacement [11–13]. A number of wastes would be generated in widespread applications. Evaluating the circularity of PSC technology is vital for its large-scale integration into vertical building facades [14]. Fortunately, preliminary recycling methods for PSCs have been established, employing both layer-by-layer and one-step approaches [15]. Also, Gallegos et al. [16] showed that employing two environmentally friendly solvents in a room-temperature process with brief exposure times can effectively dissolve the different layers of PSCs, allowing for the recovery of the ITO substrate. An introduced procedure facilitates the individual removal of each layer of the PSCs, allowing for selective isolation of different materials [17]. This simple recycling method effectively reduces the risk of contamination and addresses waste disposal challenges, while also contributing to overall cost reduction within the system. Li et al. [18] demonstrated that recycling PSC materials can yield significant economic benefits.

1.2. Economic analysis for photovoltaic façade

To prove application potential for buildings, the economic feasibility of photovoltaic façade should be investigated firstly. There are three steps for the investigation: modeling 3D buildings, analyzing solar radiation access, and conducting lifecycle cost analysis (LCCA). In many regions, access to urban data for 3D modeling remains challenging, with accurate dimensional data for buildings often unavailable. Consequently, modeling 3D buildings poses a significant obstacle [19]. Researchers employed theoretical calculations [20], on-site tests [21,22], and simulation tools [23,24] to investigate solar radiation access for BIPV systems. For the on-field test, long test time is required. For most of modeling and theoretical calculations, an issue is that the analyses do not consider the influence of the shadow caused by surrounding structures. It can cause large errors in the results especially in dense cities, leading to overestimation of profits in the LCCA calculation. Accurate analysis of solar radiation depends on an accurate environmental model. An efficient 3D modeling approach is required to realize rapid and accurate solar radiation analysis. So, this study uses grasshopper ladybug to assess the solar radiation of the PSC façade, considering the influence of the shadow in the studied district. An efficient 3D modeling approach is proposed to generate editable building models to tremendously reduce the labor cost for manually access the building information.

LCCA is a lifecycle tool that specifies the expected cost of producing, transporting, using, and disposing of a product or service [25]. LCCA enables the financial evaluation of the BIPV project, depending on criteria to achieve the lowest cost and largest profit. An investigation is one that enables end-users to select the energy for the buildings while taking into account the repercussions of their choice. The analysis is intended to assess a variety of accessible solutions, like various BIPV systems due to dual purpose as building skins and power generator. Also, advancements in recycling technology have led to the creation of innovative methods for conducting LCCA with a focus on circular economy principles.

The analysis of solar radiation plays a pivotal role in calculating the economic performance of BIPVs. Additionally, numerous economic indicators are employed to illustrate the economic viability of such systems. Sow et al. [21] investigated the economic feasibility of BIPV projects, employing the discounted cash flow method and fundamental economic principles. D'Adamo et al. [26] assessed the impact of subsidies on the BIPV market in Italy, particularly focusing on the reinstatement of subsidies for PV plants, employing a discounted cash flow methodology. Olivieri et al. [23] explored the advantages of introducing PV Distributed Generation at campus using PVSyst. Gholami et al. [27] conducted a LCCA of a BIPV vertical envelope based on four years of on-field data collected from 2016 to 2019. The LCCA considered benefits earning from energy production and three component recycling methods. Some studies also investigated the economic feasibility of PSC façade in recent years. Li et al. [25] explored the use of PSCs integrated into textile envelopes for building energy supply and assessed the economic feasibility of the system. The results indicated that PSCs have significant potential for financial benefits in BIPV applications. Table 1 shows the literature published in last 5 years, along with the main results. Most of BIPV systems in previous studies are in the environment without too much shadow. The economic feasibility of PSC façade in dense urban environments is rarely investigated, which significantly impacts their adoption and diffusion.

Herein, this study will investigate economic feasibility of circular PSC façades in dense urban environment using a novel 3D modeling approach and LCCA. The rest of paper is as following structure: In Section 2, the methodology framework is provided, including the 3D modeling process, building performance analysis, and life cycle cost analysis; Section 3 presents the case study description; In Section 4, the results of modeling and economy analysis are presented; Discussion is shown in Section 5, and a conclusion is provided in the end.

2. Methodology

There are four main parts in the framework: aerial video-based 3D modeling, building performance simulation, LCCA, and multi-objective optimization shown in Fig. 1. The details are discussed in this section (see Fig. 2).

2.1. 3D modeling

The initial step is to use 3D reconstruction method LCM-MVSNet to generate the point cloud model based on aerial video of the target district [31,32]. Following this, the point cloud model is imported into Rhino, where noise removal is conducted by trimming the model. Subsequently, building boundaries are identified and building surfaces can be modelled based on the point cloud data. The approach realizes 3D modeling.

Table 1
Overview of existing economic feasibility studies of BIPV systems.

Year	Location	Simulation	Economic indicator	Reference
2019	Canada	Test	DPP	[21]
2020	Italy	Test	NPV	[26]
2020	Madrid, Spain	PVSyst	NPV, IRR, DPP	[23]
2020	Solsmaragden, Norway	Test	NPV, DPP, IRR, LCOE	[27]
2021	Abruzzo, Italy	Proger SpA	NPV, DPP.	[28]
2022	Zurich, Switzerland	Theoretical calculation	DPP	[20]
2022	Melbourne, Australia	Revit	NPV, DPP, LCOE	[14]
2023	Milan, Italy	Theoretical calculation	NPV, DPP, IRR, LCOE	[9]
2024	Norway	Test, PVSyst	LCOE	[29]
2024	Italy	PV-GIS	LCOE	[30]
2024	Solsmaragden, Norway	Theoretical calculation	NPV, DPP, IRR, LCOE	[18]

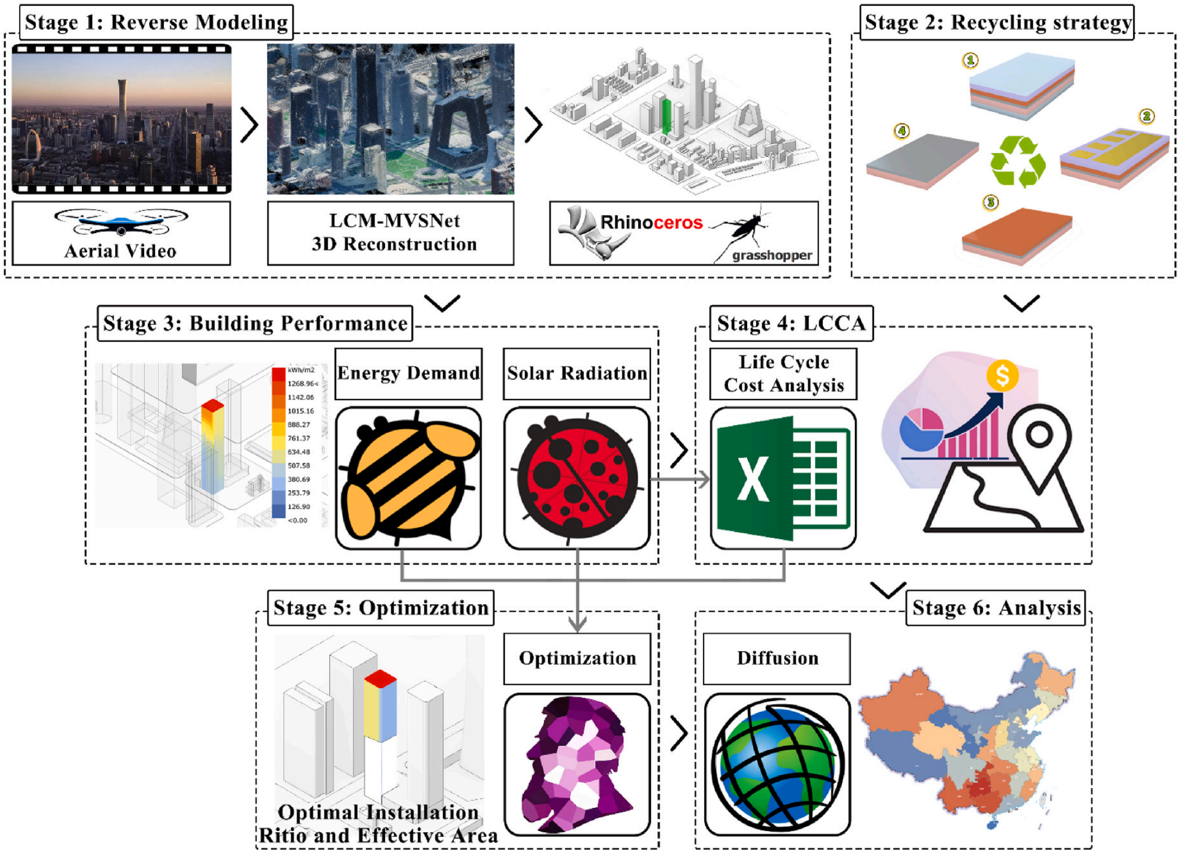

Fig. 1. Framework for the calculation of economic feasibility of the PSC façade.

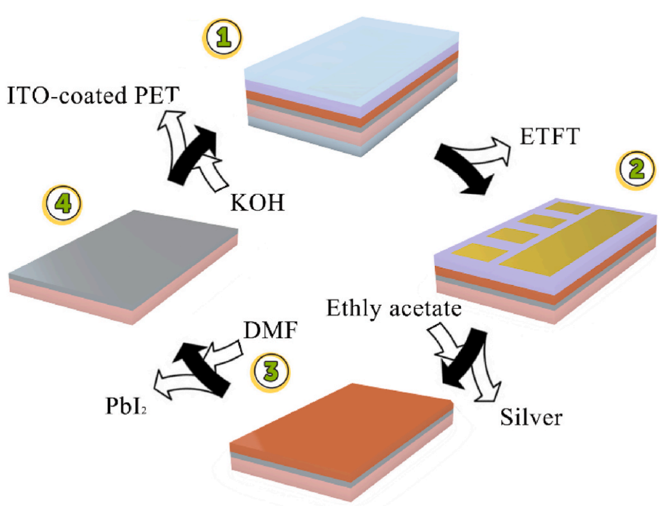

Fig. 2. 4 steps for PSC recycling.

2.1.1. *3D reconstruction of the site*

Our research group develops LCM-MVSNet to create the 3D model of the surrounding environment of the target building. LCM-MVSNet is a two-stage deep learning-based method for automated point cloud reconstruction by using drone photography. The details are shown here.

Firstly, it is to finalize depth inference. For feature pyramid extraction network, multi-view images $\{\mathbf{I}_i\}_{i=0}^{N}$ are provided. (L+1)-level features $\left\{\mathbf{f}_{l,i} \in \mathbb{R}^{F_l \times H/2^l \times W/2^l}\right\}_{l=0}^{L}$ can be obtained for each image $\mathbf{I}_i$, where F_l is the channel number. Next, the image features and camera parameters are required to encode into the network. At level l, a uniform sampling method is used to create (M_l + 1) depth hypotheses throughout the space. The hypotheses are drawn from the depth range [$d_{\min,l}$, $d_{\max,l}$] defined by the reference camera's viewing frustum. Features from the source perspective are generated in the space using the sampled depth hypotheses through homography transformation. This process warps image features extracted from the source perspective into the reference camera's frustum, constructing features in the (N+1) perspective. To store the input views, the cost volumes of the (N + 1) perspective are consolidated to a unified volume $\mathbf{C} \in \mathbb{R}^{F_{l,c} \times M_l \times H/2^l \times W/2^l}$ to measure the corresponding degree of multi-view features.

2.1.1.1. *Learnable cost metric.*

The Learnable Cost Metric (LCM) at level l is shown as:

$$\begin{aligned} \mathbf{C}_l &= M\left(\mathbf{V}_{l,o}, \cdots, \mathbf{V}_{l,N}\right) \\ &= M\left(\mathbf{B}_{l,o}, \cdots, \mathbf{B}_{l,N}\right) \\ &= AvgPool\left(\alpha_l \mathbf{B}_{l,0} \odot \sum_{i=1}^{N} \frac{S_i}{\sum_{i=1}^{N} S_i} \mathbf{B}_{l,i}\right) \end{aligned} \tag{1}$$

Where $\mathrm{B}_{l,i} \in \mathbb{R}^{K \times (F_l/K) \times M_l \times H/2^l \times W/2^l}$ stands for stands the batched volumes after evenly separating the original volumes $\mathbf{V}_{l,i}$ into K batches along the channel dimension. $\mathbf{V}_{l,i}$ into K batches along the channel dimension. Additionally, the normalized matching score $S_i/\sum_{i=1}^{N} S_i$ is applied as the source-view significance. $\odot$ stands for the Hadamard product.

To regularize the cost volume and estimate the depth, a convolutional neural network is used to regularize the aggregated cost volume pyramid $\{\mathbf{C}_l\}_{l=0}^{L}$ and create the probability volume pyramid $\{\mathbf{P}_{l,est}\}_{l=0}^{L}$ using the sigmoid activation function. The refinement of the discrete depth estimation involves adjusting for the estimated discrepancy between the actual target depth and the initial discretized depth values:

$$\mathbf{D}_{l,est} = \underset{dm,l_{\in[d\ min,l,d\ max,l]}}{\operatorname{argmax}} \mathbf{P}_{l,est}(d_{m,l}) + \frac{(d_{max,l} - d_{min,l})}{M_l} \max \mathbf{P}_{l,est}(d_{m,l}) \tag{2}$$

where $\underset{dm,l_{\in[d\ min,l,d\ max,l]}}{\operatorname{argmax}} \mathbf{P}_{l,est}(d_{m,l})$ is the discrete depth. $(d\,max, l - d_{min,l}) / M_l$ is the depth interval. $\max \mathbf{P}_{l,est}(d_{m,l})$ is the normalized bias.

In training the network, focal loss is employed to directly supervise the probability volume, enhancing the model's ability to focus on hard-to-classify examples (Li, X. et al., 2020; Lin et al., 2017).

The second stage involves generating the point cloud using the depth map filtering and fusion strategy. Depth map fusion is performed to merge the inferred multi-view depth maps $\{\mathbf{D}_i\}_{i=0}^{N}$. During the filtering of depth maps, a probability threshold τ is established to remove depth outliers and define the number of consistent views N_c to address depth inconsistencies. The photometric constraint evaluates the matching quality of the multi-view depth maps, while the geometric constraint assesses their consistency. Subsequently, the refined depth maps are merged to produce the final point cloud.

2.1.2. 3D model generation

The point cloud model, generated through LCM-MVSNet, serves as the input to Rhino. Currently, the conversion of a point cloud to NURBS surfaces within Rhino is challenging, particularly in complicated and cluttered building environments. However, for the purpose of assessing solar radiation on the PSC facade, the critical information required pertains solely to the dimensions, form, and relative positions of the buildings. As such, this study adopts an approach focused on identifying building boundaries and control point [33]. Initially, the point cloud data undergoes importation into Rhino to eliminate noise points. Subsequently, the "Resurf" module is used to convert the point cloud into a mesh. Following this, "single surface from mesh" is applied with 'Max Tol' set to 0.5 and 'Smooth' set to 'medium,' resulting in the generation of a NURBS surface. However, the uneven and defective surfaces generated from above operations cause many bumps and projections in the model, which cannot be directly used for the solar radiation simulation. But this step transforms the colorful point cloud into rendered mesh where the profile of the buildings can be easily identified for subsequent operations in the Rhino interface. Next, boundary lines are extracted from mesh. The control points can be selected from the boundary lines for modeling the building surfaces. Finally, a distance between these two points in the real world is measured as the reference for the actual dimension of the model.

2.2. Building performance simulation

Grasshopper serves as a visual scripting platform embedded in the Rhinoceros 3D computer-aided design application, facilitating the evaluation of performance through algorithmic processes. The fundamental components of the Grasshopper-based investigation comprise three integral sections: model creation, performance simulation, and data output. Notably, solar radiation is calculated utilizing Ladybug and building energy demand is calculated by Honeybee.

For the solar radiation, Ladybug employs Radiance's GenCumulativeSky algorithm to generate sky matrix patch values derived from a weather file. This process facilitates the computation of radiation received by the building facades at each hour throughout the year. The outcomes manifest in the form of visually interpretable colored mesh representations. PSCs are integrated into varying proportions of the building facade, specifically at percentages of 20 %, 40 %, 60 %, 80 %, and 100 %. This variation is implemented to evaluate and determine the optimal integration percentage. For indoor lighting, spatial daylight autonomy (sDA) represents the proportion of the building area where the illuminance level equals or surpasses 300 lux for a minimum of 50 % of daylighting hours (8–18 o'clock) annually. It is also calculated by Ladybug.

For the building energy demand, Honeybee is a plugin tool in the grasshopper based on EnergyPlus. The installation of PSCs on the vertical glazing façade influences the building heat gain. The building function for the block is uniformly set as office buildings. The parameter settings primarily align with Chinese building codes.

2.3. Life cycle cost analysis

The LCCA is primarily used to figure out the viability of new products. In this study, it serves as the tool for evaluating the economic viability of the target PSC facade. The investigating scope of the LCCA spans from 2021 to 2050.

2.3.1. Life cycle cost

Initial investment consists of the material cost and personnel cost. The expenses associated with PSCs, inverters, and other components are collected. Given the absence of commercial PSC panels on the market, the cost of PSCs is derived from selling price forecasts. Notably, in this study, it is assumed that the PSCs are produced in a large-scale local factory. The price for the PSC is intricately linked to the purchasing amount of PSC and follows the model proposed in the literature (Mathews et al., 2020). The personnel, electricity, equipment, and other costs are set as 20 % of the total material cost based on the project conducted by company Heliatek. Heliatek produces organic solar cells, which have similar physical characters with PSCs. Therefore, the experience in their products is introduced as a reliable reference. The costs for the aforementioned materials are provided in Table 2.

Operation and maintenance (O&M) cost is allocated for sustaining the daily operation of the PSC facade. According to the BIPV project implemented in Ruichang E-commerce Center, where the O&M expenditure amounts to approximately 0.5 % of the initial cost per annum. This study adopts the same O&M cost percentage for the LCCA study.

Non-O&M cost includes taxes, insurance, etc. The PSC facade discussed in this paper aligns with the income tax rate of 25 % applicable to non-main power generation enterprises. Given the susceptibility of PSC facade operations to the impact of unpredictable factors such as extreme weather and natural disasters, it is customary to mitigate risks through insurance coverage. An annual insurance fee equivalent to 0.25 % of the initial investment is considered a prudent measure for stabilization and loss prevention [34].

Table 2
Parameters of the BIPV project for the economic analysis.

Parameter	Value	Unit
Site	Beijing, China	
PSC price	4.28RMB/W for 3.14 MW purchasing 4.33RMB/W for 2.62 MW purchasing 4.41RMB/W for 1.97 MW purchasing 4.53RMB/W for 1.31 MW purchasing 4.68RMB/W for 0.66 MW purchasing	RMB/W
Personnel, equipment, and other cost	20 %	
PSC PCE	12 %	
O&M cost	0.5 %	
Insurance cost	0.25 %	
Inverter replacement cost	10 %	
Transmission line lost power	6 %	
Power delivery cost	20 %	
Electricity price	0.49	RMB/kWh
Electricity tariff inflation rate	2.5 %	
Discount rate	2.6 %	

Replacement cost includes both the inverter and PSC replacements [35], with the assumption that the replacement price equals the initial purchase price in the first year.

2.3.2. Investor income

Electricity sale income stands as a crucial component, influenced by both electricity production and the local electricity price prevailing in the market. For a grid-connected BIPV project, the electricity price (including taxes) is established at 0.49 RMB/kWh in 2023. The provided report indicates a year-on-year increase of 2.5 % in the electricity price. Consequently, this study adopts a growth rate of 2.5 % for the electricity price.

Recycling benefits stands as the value of BIPV systems in the End-of-Life (EOF) phase by recycling the layers of PSCs. Recycling PSCs can reduce the financial pressure of investor and enhance the sustainability of the building sector. Specifically, the direct bonding of PSC panels to the vertical envelope fosters recyclability by eliminating the need for substructure materials required for silicon PV cells. This study applies a common cell architecture proposed in Ref. [36] and includes the silver front electrode, Spiro-OMeTAD, perovskite layer, ITO electrode, PET substrate, and final encapsulation barrier ETFE. This reduction in material diversity within the multi-material composite contributes to a more streamlined recycling process. A novel and realizable recycling process is conducted in TU Delft. The details (Fig. 3) are shown as the following steps:

Step 1 is to peel off the ETFE foil mechanically. Next, the silver front electrode is first detached using ethyl acetate, then filtered to separate the silver. The substrate is subsequently removed from the solution and dried under a nitrogen stream. Step 3 is to reconverted the perovskite layer into PbI_2 and methylammonium iodide (MAI) through a brief immersion in double-distilled water. Subsequently, after removing MAI from the water, the materials are dried using a nitrogen stream. The substrate is subsequently placed on a 100 °C hotplate for 10 min to ensure all residual water is evaporated. PbI_2 is removed from the substrate by putting the sample in dimethylformamide. The process concludes with treating the samples in a 1.5 M potassium hydroxide solution and subsequently rinsing with deionized water to recover the ITO-coated PET.

Cost analyses present the significance of ITO-PET as a primary factor influencing the cost of solar cells. In the work, the cost assessment outlined in Table 3 shows that ITO-PET stands as the most substantial contributor to the overall cost of PSCs. Spiro-OMeTAD is also identified as a notable cost factor; but recent research indicates the potential for low-price materials as alternative of Spiro-OMeTAD, thereby diminishing the criticality of recycling Spiro-OMeTAD. Conversely, the perovskite layer, including PbI_2 and MAI, constitutes a comparatively minor portion of the total PSC cost. Moreover, the contribution of silver electrodes is minimal due to the low silver content per square meter. The overall recycling rate is set as 80 % based on the experiments. The corresponding recovery prices for materials are detailed in Table 4.

Power distribution benefits lie in the cost saving related to the power transmission line and delivery systems with the application of PSC facades.

2.3.3. Social benefits

Transmission line lost power refers to the energy dissipated during long-distance transmission from the grid to the user. However, this concern is mitigated in the case of the PSC facade, as the generated energy can be utilized for the building's operations [39]. Based on World Bank Data, the electricity transmission loss in China is reported to be 5.26 %.

Power delivery cost refers to the costs associated with the infrastructure constructed and maintained for the transmission of electricity [40]. In contrast, the installation costs of PSC facade are directly on the building, leading to a substantial reduction infrastructure construction. Typically, power delivery costs constitute approximately 20 % of the electricity price.

Table 3
The benefits of materials recycled from the PSC.

	Recycling benefits (RMB/m^2)	Source
ITO-coated PET	154.3	Mianyang Prochema Commercial Co., Ltd.
Perovskite	5.6	[37]
Ag electrodes	3.0	[38]
ETFE foil	93.7	[38]

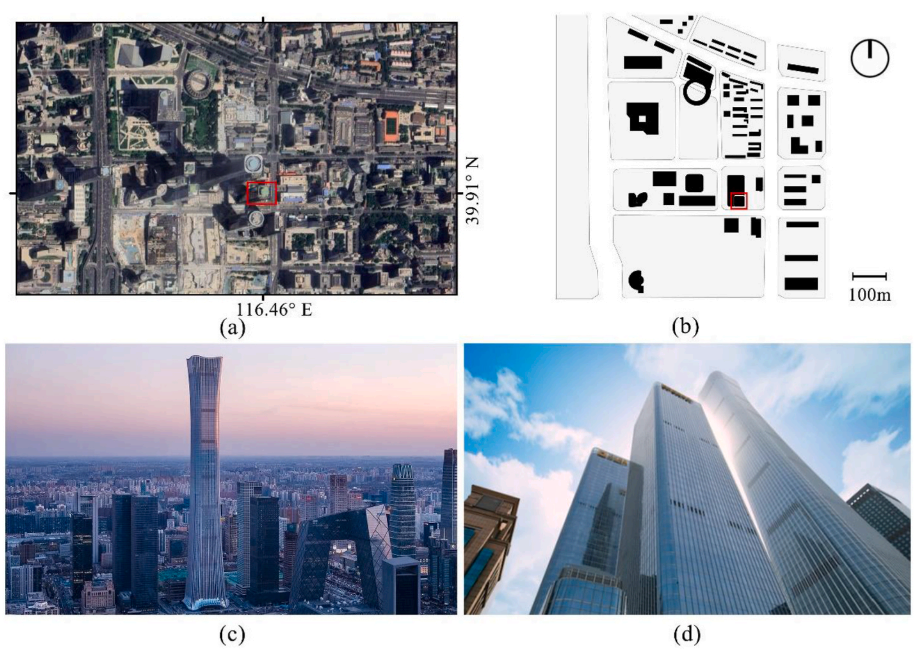

Fig. 3. Building information. (a) (b) Location of the Zhengda Center. (c) Aerial view of the district. (d) Zhengda Center.

Table 4
Cost of input materials for the recycling.

	Price for 10 MW	Amount ($/m^2$)	Price (RMB/m^2)	Source
Ethyl acetate	160.2 RMB/L	0.02 L	2.6	Sigma-Aldrich Shanghai Co Ltd
DMF	70 RMB/kg	2.9 g	0.2	Sigma-Aldrich Shanghai Co Ltd
1.5M KOH	23.7 RMB/L	0.03 L	0.6	Sigma-Aldrich Shanghai Co Ltd

2.3.4. Economic indicators

In this LCCA study, the primary economic indicators utilized to depict the profitability of the PSC facade are LCOE, NPV, and DPP.

Levelized Cost of Energy stands as a pivotal economic indicator in the realm of renewable energy technologies [41]. It is essentially the ratio of investments to power generation, representing the cost per unit of energy. Typically, LCOE is assessed in comparison to the prevailing market electricity price. The formulation of LCOE is expressed by the following equation:

$$LCOE = \frac{C_L}{E_g} \tag{3}$$

where E_g stands for the electricity production in the whole life. C_L means the whole cost in the lifecycle.

$$C_L = Q_I + C_O \tag{4}$$

where Q_I means the initial investment and C_O is the cash outflows. C_O of the system in year i can be calculated by the follow:

$$C_{Oi} = C_{OMi} + C_{Ri} \tag{5}$$

where C_{OMi} stands for the O&M costs and C_{Ri} stands for the investment for equipment replacement in the i year.

Net Present Value is an important financial metric that signifies the net advantages throughout the life of one project. It is determined by subtracting the total costs incurred over the project's lifespan from the present value of its benefits. Calculation method is expressed as following equation:

$$NPV = \sum_{1}^{n} (C_I - C_O)(1 + D_R)^n \tag{6}$$

where C_I stands for the cash inflows. D_R stands for the discount rate and n stands for the lifespan of the PSC façade. The discount rate represents the interest rate [42]. This work sets the real D_R at 2.6 %.

This study uses two NPV methods: traditional NPV and comprehensive NPV. The traditional NPV considers life cycle cost and investor income. Besides the two parts, the comprehensive NPV method extends its purview to include social benefits (transmission line lost power saving and power delivery cost saving) to show the economic performance based on the view of the society. The comprehensive NPV is to assist decision-makers in comprehending the overall benefits of BIPV projects within the broader context of the country. A noteworthy scenario arises wherein the traditional NPV is negative, signifying that the property owner may not accrue individual profits. However, the comprehensive NPV is positive, indicating societal or administrative area benefits. In such cases, the project is incentivized and advanced through government subsidies to align with broader societal goals.

Discounted payback period is a commonly used metric that measures the time needed for a system to recover the full initial investment. It quantifies the number of years required for the net cash flow to match the initial expenditure. The calculation method is presented as the following equation:

$$\sum_{i}^{n} (C_{Ii} - C_{Oi})(1 + D_R)^{-n} = Q \tag{7}$$

where C_{Ii} and C_{Oi} mean the cash inflow and outflow in the i year.

2.4. Pareto optimization

Genetic algorithms have found extensive application in addressing multi-objective building performance optimization challenges within parametric modeling platforms. This study employs the NSGA-II algorithm, available through the Wallacei plugin, for multi-objective optimization tasks. NSGA-II stands as a well-regarded evolutionary algorithm utilized for multi-objective optimization tasks. This algorithm integrates a rapid non-dominated ranking method, which effectively mitigates computational complexity and enhances solution efficiency. By integrating crowding computation and an elite retention strategy, NSGA-II meticulously selects individuals to ensure the retention of the finest solution from each generation for the subsequent iteration. As a result, NSGA-II yields a varied and top-tier population of solutions, closely approximating the Pareto optimal frontiers.

The PSC is a kind of semi-transparent foil whose installation influences the indoor heat obtain and lighting of the building. This study aims to explore the solutions using multi-objective optimization algorithms while ensuring reducing LCOE, increasing indoor daylighting distribution performance, and reducing building energy demand. A MOO approach is used and the objective functions are defined as follows:

$$f_1(\varpi\%, \eta\%) = \text{Min}(LCOE) \tag{8}$$

$$f_2(\varpi\%, \eta\%) = \text{Max}(sDA) \tag{9}$$

$$f_3(\varpi\%, \eta\%) = \text{Min}(EUI) \tag{10}$$

where EUI represents energy use intensity of the building and sDA represents spatial daylight autonomy. PSC installation ratio $\omega\%$ and PV effective area $\eta\%$ are defined as variables. The investment is a constant value. Since a MOO approach is employed, the three objective values are treated as independent and are not subject to any weighting effects.

3. Case study

Beijing is one of most dense urban cities in the world. Zhengda Center, situated in the Beijing at coordinates 39.91° N, 116.46° E, is a representative commercial building in dense central business district (CBD) (Fig. 3 and Table 5). Comprising two office towers, each soaring to a height of 238 m, this super high-rise complex plays a pivotal role in the daily operations of the CBD. Given the substantial energy requirements for the buildings, the implementation of PSC facades emerges as a potential solution to curtail energy consumption and alleviate financial burdens. For the purpose of this study, one of the two buildings within Zhengda Center is selected as the focal point. This choice aims to assess the feasibility and viability of integrating PSC facades in a modern city setting in China. Notably, the selected building features vertical surfaces entirely covered by glazed facades, offering an ideal canvas for the seamless integration of PSCs. The PSCs are affixed

Table 5
Project 'Tower 1 of Zhengda Center' information.

Project Data	
City	Beijing, China
Location	39.91° N, 116.46° E
Building function	Commerce and office complex
BIPV installation position	Vertical façade
Height	238 m
Façade area	37392 m^2

directly to the glass facades using a backside adhesive. The study assumes the identification of a suitable adhesive through comprehensive testing, including accelerated aging tests. The four vertical façades of the building are all integrated PSC foils. The façade area available for PSC integration 37392 m^2.

This study contemplates the retrofitting of a vertical PSC facade. The PSC is designed as 20 %, 40 %, 60 %, 80 %, and 100 % of the building area from the top. In the study, the PCE of PSCs is conservatively estimated at 12 %. We conduct some preliminary calculations for the economic viability of PSC facades across varying PSC lifespans. It reveals that a 5-year lifespan is generally insufficient to achieve investment payback in most regions. This suggests that a 2-year lifespan is even less feasible. However, when incorporating a recycling strategy, PSCs with a 5-year lifespan become economically viable in certain regions. Based on these results, the uncertainty surrounding the lifespan of the product prompts the consideration of three scenarios: 5, 10, and 15 years, allowing for an examination of the influence on economic viability. If the PV panels reach lifespan, all the panels are replaced.

4. Results

The results are shown in this section by illustrating the effectiveness of the reversed modeling approach to generate target buildings, the detailed LCCA results for different application scenarios of PSC facade on the target building and the feasibility of PSC facades across difference regions in China.

4.1. 3D modeling

The initial phase of the feasibility analysis involves the modeling of Zhengda Center and its surrounding structures. A previous aerial video for the district was employed for the collection of building data, extracting 243 images from diverse viewpoints. It is noteworthy that each successive image encompassed 50 % of the area covered by the preceding one. Subsequently, these images underwent processing through the algorithm detailed in Section 2.1, realizing the three-dimensional reconstruction of the buildings. The resulting point cloud model was addressed involving the removal of noise points and non-essential elements (Fig. 4b). But the top half of the highest building were not reconstructed very well because there were few shots of the tallest buildings in the video. The refined point cloud model file was then imported into Rhino, where the identification of building edges was straightforward. Utilizing these boundaries, building blocks were constructed within Rhino, as illustrated in Fig. 4c.

The accuracy of the building models was investigated. The information of Zhengda Center and CITIC Tower (China Zun, the highest building in Beijing) was obtained. So, the two buildings were selected to verify the accuracy of the 3D modeling approach. Zhengda represents the regular building form. The length of the façade and the height were compared with the true value. Table 6 respectively shows the comparison between the results of reverse modeling data and the real data for the two buildings. The surface of CITIC Tower is curved. The middle line of the east façade was extracted for the validation. 100 sample points were selected. One middle point of the line was set as coordinate system origin and their horizontal coordinates were extracted for the comparison. The mean square error (MSE) was used to evaluate the error of the curved surface. The MSE result is 4.2 %.

Table 6
Modeling accuracy.

Attributes	Modeling result	Real data	Deviation
Height (m)	239.8	238.6	0.5 %
Length 1 (m)	41.7	41.3	1.0 %
Length 2 (m)	42.4	42.1	0.7 %

4.2. Solar radiation analysis

The solar radiations incident on the facades throughout the year are computed using Ladybug in Grasshopper, as shown in Fig. 5. Various scenarios representing different percentages (20 %, 40 %, 60 %, 80 %, 100 %) of the vertical façade designated for PSC installation were examined. Observing the results, it becomes evident that the received solar radiation gradually diminishes from the top to the bottom of the building. This phenomenon is attributed to the shading effects imposed by surrounding structures. Consequently, the assessment proposed in this paper for evaluating diverse PSC deployment configurations assumes significance for investors navigating various investment strategies.

4.3. Life cycle cost analysis

Results of traditional NPV are presented in Fig. 6, providing insights into the financial gains or losses for the building owner. 80 % PSC installation area is selected to show the trends of traditional NPV. The capacity of installed PSC façade system is around 3.0M W, thus the purchase price of PSCs is 4.33 RMB/W. The investigation includes three distinct lifespans for PSC - 5 years (PSC5), 10 years (PSC10), and 15 years (PSC15). Recycling scenario of PSCs is also considered as PSC5-R, PSC10-R, and PSC15-R. The results show that the investment of six PSC façade systems is same at 13.1M RMB. Without considering PSC recycling, all PSC façades fail to realize positive returns throughout their lifecycle. The traditional NPV of PSC5, PSC10, and PSC15 is −32.9M RMB, −10.5M RMB, and −3.9M RMB, respectively. Recycling PSCs can help the investor decrease the spence of the PSC façade and make PSC facades exhibit profitability for the building owner. PSC15-R emerges as the most financially robust system among the six, achieving an impressive NPV performance of 3.5M RMB. Moreover, PSC10-R also demonstrates a net benefit at 1.4M RMB. However, PSC5-R still run a business at a 3.9M RMB loss in its lifespan.

Fig. 7 shows the calculation results for the comprehensive NPV of six different scenarios. Comprehensive NPV considers the saving from social benefits. Therefore, the comprehensive NPV is higher than the traditional NPV. Without considering PSC recycling, the analysis reveals that PSC5 and PSC10 fail to recover the total investment over its lifecycle, which is consistent with the findings of the traditional NPV analysis. They exhibit negative NPV of −27.2M RMB and −5.2M RMB, respectively. However, different from the result of traditional NPV, the

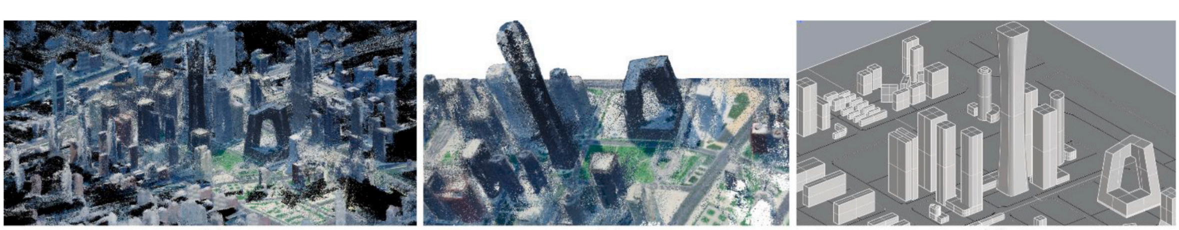

Fig. 4. Procedures of the reverse modeling. (a) 3D point could reconstruction model. (b) Trimmed model. (c) 3D district model in rhino.

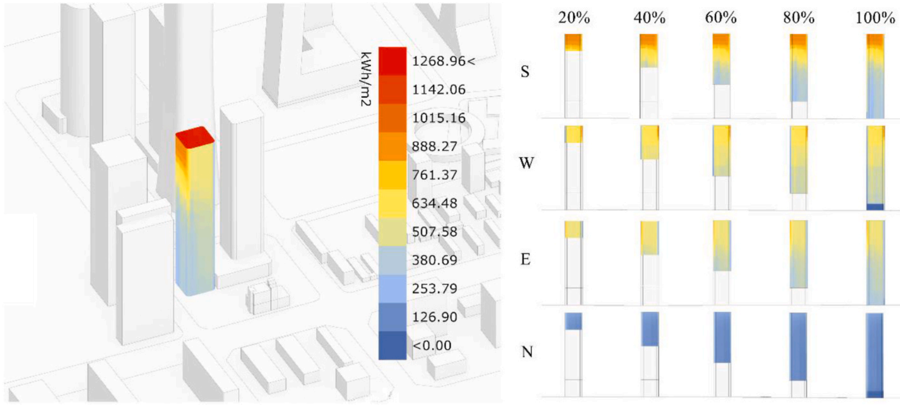

Fig. 5. Annual solar radiation of the building façades.

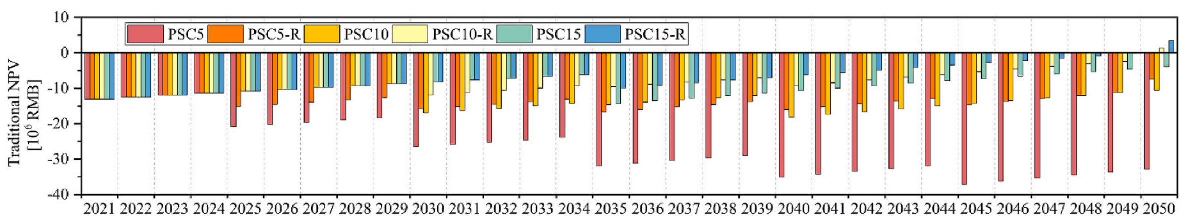

Fig. 6. Traditional NPV of the PSC façade of Zhengda Center in 30-year lifecycle in Beijing.

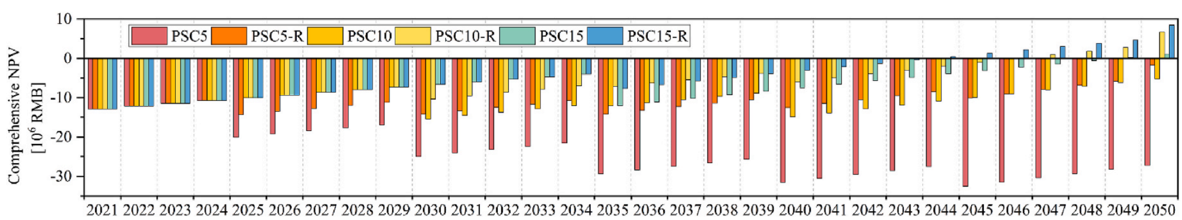

Fig. 7. Comprehensive NPV of the PSC façade of Zhengda Center in 30-year lifecycle in Beijing.

comprehensive NPV of PSC15 demonstrates the profitability, yielding a positive outcome 1.0M RMB. If considering PSC recycling, PSC15-R stands out with the highest NPV result, totaling 8.5M RMB. Following closely, PSC10-R demonstrates commendable comprehensive NPV of 6.7M RMB. The collective analysis proves the critical importance of recycling in enhancing the overall profitability of the PSC facade. As for PSC5-R, the comprehensive NPV is −1.7M RMB, which shows a sharp increase compared to its traditional NPV. Moreover, results show the social benefits account for 20 % of comprehensive NPV when the recycling strategy is not considered. The social benefits account for 5 % of

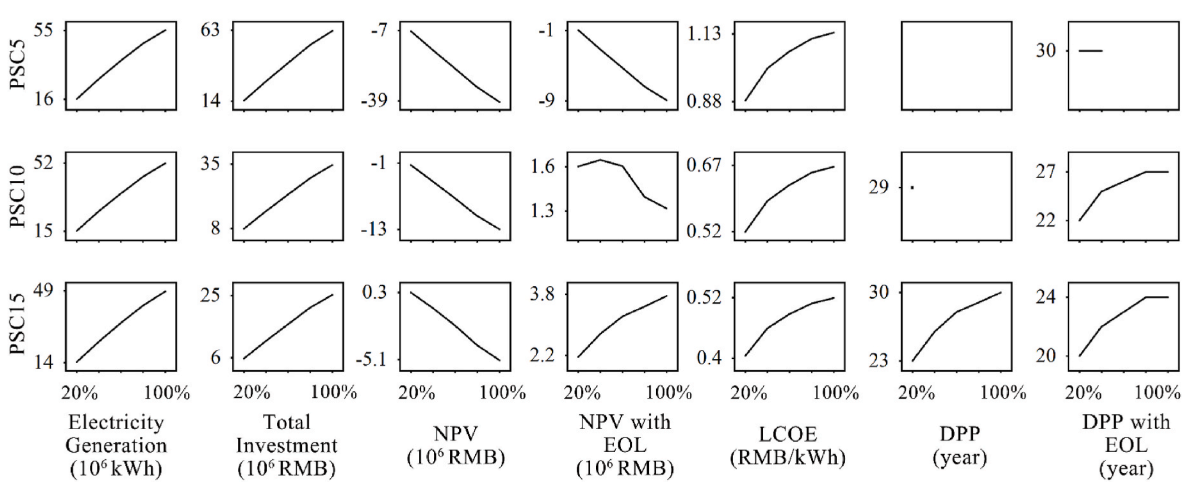

Fig. 8. The results of economic indicators for the PSC façade of Zhengda Center in Beijing. Different installation ratios (20 %, 40 %, 60 %, 80 %, 100 %) and different PSC lifespans (5, 10, 15 years) are considered.

comprehensive NPV considering recycling strategy.

The economic performance of various PSC deployment strategies (20%–100 %) is depicted in Fig. 8. The observed decline in solar irradiation from the top to the bottom of the building contributes to a diminishing slope in electricity generation as the PSC installation ratio increases. Within a consistent PSC deployment, PSC5 shows the highest investment, primarily attributable to frequent replacements. The total investment exhibits a linear growth pattern corresponding to the proportion of PSC installations. The investment range for PSC5 spans from 14M RMB to 63M RMB, while PSC10 exhibits an investment range from 8M RMB to 35M RMB. Additionally, the investment for PSC15 varies within the range of 6M RMB to 15M RMB.

The trends observed in traditional NPV reveal a linear decrease with an increase in the PSC installation ratio. The traditional NPV of PSC5 ranges from -7M RMB to −39M RMB, while PSC10 exhibits an investment range from -1M RMB to −13M RMB. Additionally, the investment for PSC15 varies within the range of 0.3M RMB to −5.1M RMB. Notably, the scenario with PSC15 and a 20 % installation ratio is the sole instance where a positive benefit is realized. Noteworthy trends in traditional NPV with EOL emerge across distinct PSC lifespans. For PSC15, traditional NPV with EOL increases with an escalating PSC installation ratio, while PSC5 and PSC10 witness a decrease in NPV with increasing installation ratios. For PSC5, the NPV shifts from -7M to −39M RMB as the installation ratio increases from 20 % to 100 %, resulting in a difference of 32M RMB. In contrast, the benefits from recycling PSC5 range from 6M to 30M RMB, which is less than the NPV variation due to installation ratio changes. On the other hand, for PSC15, the NPV changes from 0.3M to −5.1M RMB across the same installation range, with a difference of 5.4M RMB. The recycling benefits for PSC15, ranging from 1.9M to 8.5M RMB, exceed the NPV change associated with installation ratio adjustments.

As PSC installation rates increase, the slope of LCOE shows a downward trend. Furthermore, the increase in PSC lifespan correlates with a decrease in LCOE because frequent replacement of PSCs increases the investment. LCOE reaches the aforementioned lowest value when utilizing PSC15. PSC15 with 20 % installation area shows the lowest LCOE, reaching 0.4 RMB/kWh. PSC10, with a 20%–100 % installation area, demonstrates an LCOE range of 0.52–0.67 RMB, approximating the local electricity price. Conversely, PSC5 yields an LCOE range of 0.88–1.13 RMB.

For DPP, PSC5 fails to recuperate the investment. For PSC10, only 20 % installation ratio can pay back the initial investment in the 29th year. Moreover, PSC15 can achieve investment payback in any installation ratio. At 20 % installation ratio, PSC15 shows the best performance. Which can return the investment in the 23rd year. However, with a 100 % installation area, PSC15 requires 30 years to achieve payback. When considering the recycling process, PSC5 with a 20 % or 40 % installation ratio can achieve investment payback within 30 years.

From the results, a 6M RMB investment in a PSC15 facade yields 14M kWh electricity generation, translating to 2.2M RMB profits with PSC recycling. The LCOE can be reduced to 0.4 RMB/kWh. If the investor aims to maximize electricity generation, PSC5 for 100 % installation area should be selected with a 63M RMB investment, electricity generation up to 55M kWh. But it incurs a higher LCOE of 1.13 RMB/kWh. But it cannot realize a positive benefit over the lifecycle.

4.4. Pareto optimal solutions

In this section, an optimization is conducted with a total investment of 40M RMB. The optimal solutions are showed in Fig. 9. The optimization process conducted a total of 300 iterations, resulting in 104 solutions, of which 34 are identified as Pareto front solutions. Each point stands for one configuration of PSC façade. The optimal values of EUI range from 122.6 to 147.3 kWh/m^2. The optimal values of sDA range from 31 % to 49 % and the optimal values of LCOE range from 0.92 to 1.05 RMB/kWh. This multi-optimization process offers a methodology for determining the optimal configuration of PSC facades given an initial budget constraint.

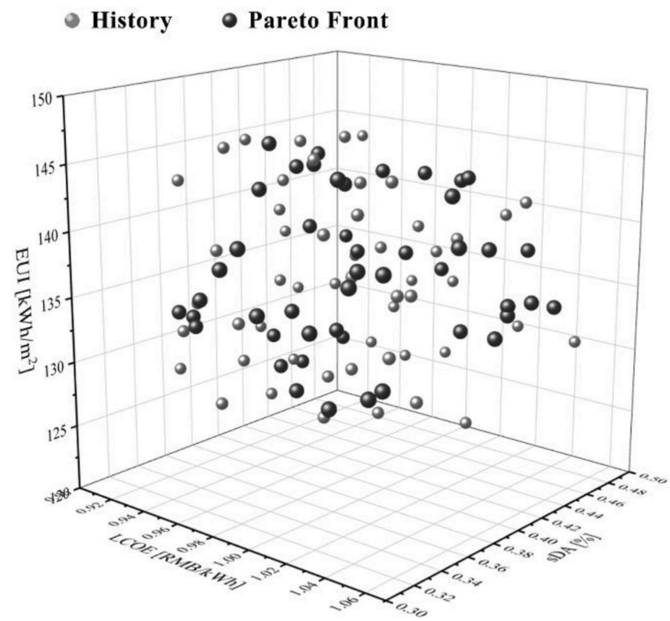

Fig. 9. Pareto front solutions and the distribution interval of the final Pareto front set objective values.

4.5. Feasibility of PSC façade in different regions of China

The sensitivity analysis conducted earlier emphasized the significant impact of solar radiation and electricity prices [43]. This phenomenon is commonly observed across various nations, with particularly pronounced effects in China for its vast territory and different energy policies in different regions with dense urban environment.

Therefore, the feasibility of PSC façade in 32 province capitals of China is also investigated. The research area focuses on the mainland, including 23 province capitals, 5 autonomous region capitals, and 4 municipalities. This study focuses on the PSC façade applied in high density urban cities. So, the province capitals in China are selected as the target cities to show the feasibility. Because the multi-objective optimization requires too much time. So, the analysis assumes a 5-year lifespan for PSCs and an 80 % installation ratio to represent the most realistic near-future scenario. Zhengda Center and Beijing CBD district planning are still used as a similar case and urban environment is assumed to exist in most province capitals. The received solar radiation of Zhengda Center in every city is simulated in Grasshopper. The electricity price of every province capital is also collected. These data are provided in the Supplementary Information.

The results are presented in Fig. 10. It can be found that the PSC façade exhibits a prominent level of energy production (58.6M–65.0M kWh) in Lasa city and Xining city. Conversely, the PSC façade in the middle regions of China demonstrate the least energy generation and the highest LCOE. The northwest region, in particular, stands out with the best LCOE performance, ranging from 0.81 to 0.97 RMB/kWh. Meanwhile, the northeast and southeast regions present intermediate LCOE levels (1.13–1.28 RMB/kWh). For the traditional NPV and comprehensive NPV, the PSC façade fails to achieve profitability in any of the cities examined. But if considering the recycling of PSCs, except Naning city and Guiyang city, positive traditional NPVs can be realized in other cities. Notably, Lanzhou city shows the most favorable performance, reaching 12.6M RMB. Although the PSC façade in Urumqi city shows relatively high electricity generation, the NPV remains low due to the city's lower electricity price. The results in Urumqi city demonstrate that high solar radiation is not the only factor for the feasibility of PSC façade

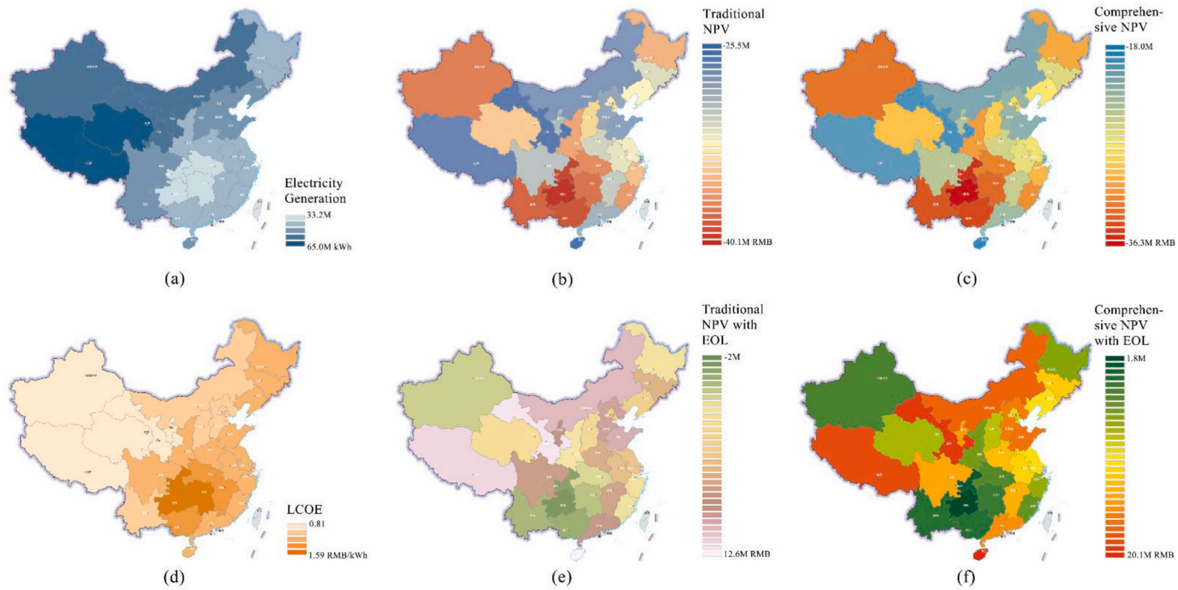

Fig. 10. The results for PSC façade in major metropolises in China.

application. Electricity prices are also crucial considerations. For comprehensive NPV with EOL, PSC façade proves profitable in all cities, highlighting the pivotal role of PSC recycling in enhancing the overall profitability of the façade system.

5. Discussion

This study also provides a novel 3D modeling approach to solve the labor-intensive manual work required in the modeling phase in urban renovation scenarios. This approach captures district-scale data from the aerial video replacing time consuming and labor-intensive modeling tasks. But the approach proposed in this work has some limitations. The approach can only provide the dimensions, shape, and relative position of individual buildings. But for the detailed building elements, such as windows and shading, cannot be identified directly from the videos and built in the model. So, this approach is not suitable for the research requiring refined modeling. In the modeling process, it is also found that this approach is easy to establish a 3D building model with a rectangular shape. However, for buildings with curved edges, more control points are required to capture the curvature accurately. Therefore, further investigations are warranted to explore techniques for identifying and segmenting complex building features.

The PSC technology makes a significant progress in recent years. In the context of carbon neutral, the deployment of vertical PSC façades emerges as a crucial opportunity for the decarbonization of buildings. Identifying suitable cities for pilot projects followed by widespread diffusion to other feasible deployment regions becomes imperative. The NPV is one of the most closely monitored indicators for investors. Based on the results in Section 4, Haikou and Guangzhou in the south of China appear as promising cities for PSC façade applications. In the northern regions, Jinan and Huhehaote stand out in terms of NPV. Meanwhile, Lanzhou and Lasa exhibit notable performance in the northwest regions.

The results highlight the financial significance of the PSC recycling. Due to the short lifespan of PSCs, the PSC façade will generate a large amount of waste. An efficient recycling strategy is required to avoid pollution and realize cost reduction. Despite employing a relatively high PSC lifespan of 5 years in the calculations, the PSC façade in the case fails to recover the investment without considering PSC recycling across urban cities in China. If considering EOL scenario, most of cities can realize benefits without any subsidy from government. Therefore, the development of a recycling strategy should be synchronized with the ongoing advancements in PSC technology.

Circular PSC façade is also beneficial for the current carbon neutrality policy. In the case, the building equipped with a PSC5 façade at an 80 % installation ratio is projected to generate approximately 4758 kWh over 30 years, equivalent to reducing 4.67 tons of CO_2-equivalent emissions from hard coal-generated electricity. This highlights the substantial potential of circular PSC façades in contributing to carbon neutrality. In our future research, we will further explore and quantify the environmental benefits associated with PSC façades.

In future research, we plan to expand the current analysis by further investigating the impact of surrounding buildings' height and deployment on solar access for PV façades. While the current study focuses on existing buildings with fixed neighboring structures, we recognize the importance of exploring how variations in the height and configuration of adjacent buildings influence the potential for PV panel installation. This will involve creating dynamic models that account for the changing shadows cast by neighboring buildings at different times of day and throughout the year, particularly in dense and compact urban areas. Additionally, we aim to investigate how these inter-building effects, in combination with building height, density, and urban compactness, can be more precisely linked to the optimal placement and efficiency of PV panels on façades. This expanded analysis will help to refine our understanding of the solar potential for PV façades in complex urban environments, leading to more accurate life cycle cost assessments and deployment strategies.

On the other hand, we aim to enhance the financial modeling of PV façade systems by incorporating a more detailed analysis of the self-consumption of electricity produced and its effect on the building's overall energy performance. Specifically, we will model the proportion of electricity generated by the PV system that is consumed on-site versus exported to the grid, taking into account factors such as building occupancy patterns, energy storage systems, and time-of-use electricity tariffs. This will allow for a more accurate assessment of cash inflows, as both the savings from reduced grid energy consumption and the revenue from exporting excess electricity to the grid will be integrated into the life-cycle cost analysis. By incorporating these factors, we can provide a more comprehensive evaluation of the NPV and the financial viability of PV façades, giving a clearer picture of their economic performance over time. This approach will improve the accuracy of our investment assessments and support more informed decision-making for investors in urban PV systems.

6. Conclusions

The economic feasibility of circular PSC façades in dense urban environment was figured out based on an efficient 3D modeling approach proposed in the study. A circular strategy for PSCs was provided to reduce the cost and decrease environmental impacts. Zhengda Center in Beijing CBD was selected as the target building for the application of PSC façade and then the simulation was extended to major metropolises in China. The 3D modeling approach used LCM-MVSNet method to realize 3D reconstruction based on the aerial video. With such a novel approach, the 3D model of Zhengda Center and surrounding structures was constructed semi-automatically, significantly reducing time and labor costs in modeling tasks. The deviation between the real data and reverse modeling data is within 1 % for buildings with regular shape.

For the economic analysis, the solar radiation of the PSC facade was evaluated by Ladybug. Different PSC deployment ratios and different PSC lifespans were considered. Traditional NPV and comprehensive NPV were proposed to compare the influence of social benefits. PSCs require frequent replacement due to their short lifespan. The recycling strategy potentially reduces the 33%–39 % of the total investment. The development of a recycling strategy should be synchronized with the ongoing advancements in PSC technology. A multi-objective optimization was conducted to offer a methodology for determining the optimal configuration of PSC facades given a budget constraint.

The PSC façade (5-year PSC lifespan) can realize profitability in the most of China dense urban cities considering the PSC recycling. In Lanzhou, the net benefit is up to 12.6M RMB. Polit cities for PSC façade applications were figured out. Haikou and Guangzhou in the south of China appear as promising cities for PSC façade applications. In the northern regions, Jinan and Huhehaote stand out in terms of NPV. Meanwhile, Lanzhou and Lasa exhibit notable performance in the northwest regions. The northwest region also stands out with the best LCOE performance, ranging from 0.81 to 0.97 RMB/kWh.

The study could be instrumental for enabling further studies exploring the feasible deployment of vertical PSC façades in dense urban environments. It also provides deep insights in the potential cities for circular vertical PSC façade applications in China.

CRediT authorship contribution statement

Qingxiang Li: Writing – original draft, Methodology, Investigation, Formal analysis, Conceptualization. **Lingege Long:** Investigation. **Xinwei Li:** Investigation. **Guidong Yang:** Investigation. **Chenhang Bian:** Investigation. **Benyun Zhao:** Investigation. **Xi Chen:** Writing – review & editing, Supervision, Funding acquisition. **Ben M. Chen:** Writing – review & editing, Supervision, Funding acquisition.

Declaration of competing interest

I confirm that we have mentioned all organizations that funded our research in the Acknowledgements section of my submission, including grant numbers where appropriate. We declare that we have no commercial or associative interest that represents a conflict of interest with other people or organizations that can inappropriately influence our work entitled, "Life Cycle Cost Analysis of Circular Photovoltaic Façade in Dense Urban Environment using 3D Modeling".

Acknowledgement

This work was sponsored by the InnoHK of the Government of the Hong Kong Special Administrative Region via the Hong Kong Centre for Logistics Robotics. Appreciation is also given to the CUHK Direct Grant for Research No. 4055168and the Research Grants Council of the Hong Kong Special Administrative Region, China (UGC/FDS16/E04/21). The authors would like to highly appreciate the help of Mr. Haoxu Wang of TU Delft for the PSC recycling process.

Abbreviations

ACVA	Adaptive cost volume aggregation	n	Lifespan of the PSC façade
B	Batched volume	NPV	Net present value
BIPV	Building Integrated Photovoltaic	NURBS	Non-Uniform Rational Basis Splines
C	Cost volume	**P**	Probability volume pyramid
CBD	Central business district	p	Pixel
C_I	Cash inflows	PCE	Power conversion efficiency
C_O	Cash outflows	PET	Polyethylene terephthalate
CNN	Convolutional neural network	P_l	Predicted probability volume
D	Depth map	$P_{l,gt}$	Ground-truth probability volume
DPP	Discounted payback period	PSC	Perovskite solar cell
D_R	Discount rate	PV	Photovoltaic
EOF	End-of-Life	sDA	Spatial daylight autonomy
ETFE	Ethylene tetrafluoroethylene	SDGs	Sustainable development goals
EUI	Energy use intensity of building	UAV	Unmanned aerial vehicle
I	Image	α	Learnable parameter
IRR	Internal rate of return	β	Tunable balancing
ITO	Indium tin oxide	λ	Loss weight
O&M	Operation and maintenance	γ	Focusing parameter
LCCA	Lifecycle cost analysis	$\eta\%$	PV effective area
LCOE	Levelized cost of electricity	$\omega\%$	PSC installation ratio
MAI	Methylammonium iodide	$\mathbb{R}$	Real number set
MOO	Multi-objective optimization	Γ	Total loss
MSE	Mean square error	$\odot$	Hadamard product
MVS	Multi-view stereo		

Appendix A. Supplementary data

Supplementary data to this article can be found online at https://doi.org/10.1016/j.renene.2024.121914.

References

[1] United Nations, Sustainable Development Goals, 2024.
[2] A.M. Shirazi, Z.S. Zomorodian, M. Tahsildoost, Techno-economic BIPV evaluation method in urban areas, Renew. Energy 143 (2019) 1235–1246, https://doi.org/10.1016/j.renene.2019.05.105.
[3] Q. Li, A. Zanelli, A review on fabrication and applications of textile envelope integrated flexible photovoltaic systems, Renew. Sustain. Energy Rev. 139 (2021) 110678, https://doi.org/10.1016/j.rser.2020.110678.
[4] L. Zhu, Q. Li, M. Chen, K. Cao, Y. Sun, A simplified mathematical model for power output predicting of Building Integrated Photovoltaic under partial shading conditions, Energy Convers. Manag. 180 (2019) 831–843, https://doi.org/10.1016/j.enconman.2018.11.036.
[5] Q. Li, L. Zhu, Y. Sun, L. Lu, Y. Yang, Performance prediction of Building Integrated Photovoltaics under no-shading, shading and masking conditions using a multi-physics model, Energy 213 (2020) 118795, https://doi.org/10.1016/j.energy.2020.118795.
[6] Y. An, J. Kim, H.-J. Joo, W.-J. Lee, G. Han, H. Kim, et al., Experimental performance analysis of photovoltaic systems applied to an positive energy community based on building renovation, Renew. Energy 219 (2023) 119369, https://doi.org/10.1016/j.renene.2023.119369.
[7] J. Čurpek, M. Čekon, Climate response of a BiPV façade system enhanced with latent PCM-based thermal energy storage, Renew. Energy 152 (2020) 368–384, https://doi.org/10.1016/j.renene.2020.01.070.
[8] Utmolight, UtmoLight Starts Building the World's First 1GW Perovskite Production Line, 2023.
[9] Q. Li, C. Monticelli, A. Kutlu, A. Zanelli, Feasibility of textile envelope integrated flexible photovoltaic in Europe: carbon footprint assessment and life cycle cost analysis, J. Clean. Prod. 430 (2023) 139716, https://doi.org/10.1016/j.jclepro.2023.139716.
[10] R.J. Yang, S.T. Imalka, W.M.P. Wijeratne, G. Amarasinghe, N. Weerasinghe, S.D. S. Jayakumari, et al., Digitalizing building integrated photovoltaic (BIPV) conceptual design: a framework and an example platform, Build. Environ. 243 (2023) 110675, https://doi.org/10.1016/j.buildenv.2023.110675.
[11] F.-W. Liu, G. Biesold, M. Zhang, R. Lawless, J.-P. Correa-Baena, Y.-L. Chueh, et al., Recycling and recovery of perovskite solar cells, Mater. Today 43 (2021) 185–197, https://doi.org/10.1016/j.mattod.2020.11.024.
[12] Q. Li, C. Monticelli, A. Zanelli, Life cycle assessment of organic solar cells and perovskite solar cells with graphene transparent electrodes, Renew. Energy 195 (2022) 906–917, https://doi.org/10.1016/j.renene.2022.06.075.
[13] Q. Li, M.R. Vogt, H. Wang, C. Monticelli, A. Zanelli, Life cycle assessment of roll-to-roll produced chemical vapor deposition graphene transparent electrodes towards copper foil recycling, J. Clean. Prod. 468 (2024) 143068, https://doi.org/10.1016/j.jclepro.2024.143068.
[14] W.M.P.U. Wijeratne, T.I. Samarasinghalage, R.J. Yang, R. Wakefield, Multi-objective optimisation for building integrated photovoltaics (BIPV) roof projects in early design phase, Appl. Energy 309 (2022) 118476, https://doi.org/10.1016/j.apenergy.2021.118476.
[15] K. Wang, T. Ye, X. Huang, Y. Hou, J. Yoon, D. Yang, et al., "One-key-reset" recycling of whole perovskite solar cell, Matter 4 (2021) 2522–2541, https://doi.org/10.1016/j.matt.2021.05.023.
[16] M.V. Gallegos, L. Gil-Escrig, K.P.S. Zanoni, H.J. Bolink, L.C. Damonte, Recycling and reusing ITO substrates from perovskite solar cells: a sustainable perspective, Sol. Energy Mater. Sol. Cell. 277 (2024) 113117, https://doi.org/10.1016/j.solmat.2024.113117.
[17] H. Zhang, N.-G. Park, Towards sustainability with self-healing and recyclable perovskite solar cells, eScience 2 (2022) 567–572, https://doi.org/10.1016/j.esci.2022.11.001.
[18] Q. Li, Z. Chen, X. Li, S. Brancart, M. Overend, Vertical perovskite solar cell envelope for the circular economy: a case study using life cycle cost analysis in Europe, J. Clean. Prod. 467 (2024) 143017, https://doi.org/10.1016/j.jclepro.2024.143017.
[19] G. Yang, X. Zhou, C. Gao, X. Chen, B.M. Chen, Learnable cost metric-based multi-view stereo for point cloud reconstruction, IEEE Trans. Ind. Electron. (2024) 1–10, https://doi.org/10.1109/TIE.2023.3337697.
[20] X. Han, J. Garrison, G. Hug, Techno-economic analysis of PV-battery systems in Switzerland, Renew. Sustain. Energy Rev. 158 (2022) 112028, https://doi.org/10.1016/j.rser.2021.112028.
[21] A. Sow, M. Mehrtash, D.R. Rousse, D. Haillot, Economic analysis of residential solar photovoltaic electricity production in Canada, Sustain. Energy Technol. Assessments 33 (2019) 83–94, https://doi.org/10.1016/j.seta.2019.03.003.
[22] Q. Li, T. Li, A. Zanelli, Performance evaluation of flexible photovoltaic panels for energy supply in post-disaster emergency shelters, J. Build. Eng. (2024) 111285, https://doi.org/10.1016/j.jobe.2024.111285.
[23] L. Olivieri, E. Caamaño-Martín, L.-N. Sassenou, F. Olivieri, Contribution of photovoltaic distributed generation to the transition towards an emission-free supply to university campus: technical, economic feasibility and carbon emission reduction at the Universidad Politécnica de Madrid, Renew. Energy 162 (2020) 1703–1714, https://doi.org/10.1016/j.renene.2020.09.120.
[24] Q. Li, G. Yang, C. Bian, L. Long, X. Wang, C. Gao, et al., Autonomous design framework for deploying building integrated photovoltaics, Appl. Energy 377 (2024) 124760, https://doi.org/10.1016/j.apenergy.2024.124760.
[25] Q. Li, T. Li, A. Kutlu, A. Zanelli, Life cycle cost analysis and life cycle assessment of ETFE cushion integrated transparent organic/perovskite solar cells: comparison with PV glazing skylight, J. Build. Eng. 87 (2024) 109140, https://doi.org/10.1016/j.jobe.2024.109140.
[26] I. D'Adamo, P.M. Falcone, M. Gastaldi, P. Morone, The economic viability of photovoltaic systems in public buildings: evidence from Italy, Energy 207 (2020) 118316, https://doi.org/10.1016/j.energy.2020.118316.
[27] H. Gholami, H. Nils Røstvik, N. Manoj Kumar, S.S. Chopra, Lifecycle cost analysis (LCCA) of tailor-made building integrated photovoltaics (BIPV) façade: solsmaragden case study in Norway, Sol. Energy 211 (2020) 488–502, https://doi.org/10.1016/j.solener.2020.09.087.
[28] I. D'Adamo, F. De Monte, F. Ferella, M. Gastaldi, The case study of a photovoltaic plant located at the university of L'Aquila: an economic analysis, J. Clean. Prod. 278 (2021) 123561, https://doi.org/10.1016/j.jclepro.2020.123561.
[29] H. Gholami, Technical potential of solar energy in buildings across Norway: capacity and demand, Sol. Energy 278 (2024) 112758, https://doi.org/10.1016/j.solener.2024.112758.
[30] F. Rossi, M. Jelagat Kipyator, T. Aernouts, H. Pettersson, R. Basosi, M.L. Parisi, et al., Unveiling the potential of perovskite solar systems in building integrated installations: a consequential and prospective life cycle assessment and economic analysis, Energy Build. 312 (2024) 114214, https://doi.org/10.1016/j.enbuild.2024.114214.
[31] Q. Li, G. Yang, C. Gao, Y. Huang, J. Zhang, D. Huang, et al., Single drone-based 3D reconstruction approach to improve public engagement in conservation of heritage buildings: a case of Hakka Tulou, J. Build. Eng. 87 (2024) 108954, https://doi.org/10.1016/j.jobe.2024.108954.
[32] G. Yang, X. Zhou, C. Gao, B. Zhao, J. Zhang, Y. Chen, et al., Multi-view stereo with learnable cost metric, in: 2023 IEEE/RSJ International Conference on Intelligent Robots and Systems (IROS), IEEE, Detroit, MI, USA, 2023, pp. 3017–3024, https://doi.org/10.1109/IROS55552.2023.10341606.
[33] M. Pepe, D. Costantino, V.S. Alfio, A.G. Restuccia, N.M. Papalino, Scan to BIM for the digital management and representation in 3D GIS environment of cultural heritage site, J. Cult. Herit. 50 (2021) 115–125, https://doi.org/10.1016/j.culher.2021.05.006.
[34] Z. Yu, Z. Lu, W. Xin, H. Pu, J. Jiang, B. Ye, Environmental and economic evaluation of urban building-integrated photovoltaic and electric vehicle system, J. Build. Eng. 95 (2024) 110205, https://doi.org/10.1016/j.jobe.2024.110205.
[35] B. Zhao, X. Zhou, G. Yang, J. Wen, J. Zhang, J. Dou, et al., High-resolution infrastructure defect detection dataset sourced by unmanned systems and validated with deep learning, Autom. ConStruct. 163 (2024) 105405, https://doi.org/10.1016/j.autcon.2024.105405.
[36] R. Chang, Y. Yan, J. Zhang, Z. Zhu, J. Gu, Large-grain and smooth cesium doped CH3NH3PbI3 perovskite films by cesium iodide post-treatment for improved solar cells, Thin Solid Films 712 (2020) 138279, https://doi.org/10.1016/j.tsf.2020.138279.
[37] A. Binek, M.L. Petrus, N. Huber, H. Bristow, Y. Hu, T. Bein, et al., Recycling perovskite solar cells to avoid lead waste, ACS Appl. Mater. Interfaces 8 (2016) 12881–12886, https://doi.org/10.1021/acsami.6b03767.
[38] F. Machui, M. Hösel, N. Li, G.D. Spyropoulos, T. Ameri, R.R. Søndergaard, et al., Cost analysis of roll-to-roll fabricated ITO free single and tandem organic solar modules based on data from manufacture, Energy Environ. Sci. 7 (2014) 2792, https://doi.org/10.1039/C4EE01222D.
[39] K. Yuan, Q. Li, W. Ni, X. Lü, G. Della Vecchia, H. Wang, et al., Analysis of the structural and environmental impacts of hydrophilic ZSM-5 molecular sieve on loess, Construct. Build. Mater. 366 (2023) 130248, https://doi.org/10.1016/j.conbuildmat.2022.130248.
[40] L. Zhu, J. Zhang, Q. Li, Z. Shao, M. Chen, Y. Yang, et al., Comprehensive analysis of heat transfer of double-skin facades integrated high concentration photovoltaic (CPV-DSF), Renew. Energy 161 (2020) 635–649, https://doi.org/10.1016/j.renene.2020.07.045.
[41] L. Long, Q. Li, Z. Gan, J. Mu, M. Overend, D. Zhang, Life cycle assessment of stone buildings in the Taihang mountains of Hebei province: evolution towards cleaner production and operation, J. Clean. Prod. 399 (2023) 136625, https://doi.org/10.1016/j.jclepro.2023.136625.
[42] K. Yuan, Q. Li, W. Ni, L. Zhao, H. Wang, Graphene stabilized loess: mechanical properties, microstructural evolution and life cycle assessment, J. Clean. Prod. 389 (2023) 136081, https://doi.org/10.1016/j.jclepro.2023.136081.
[43] Q. Li, C. Monticelli, A. Kutlu, A. Zanelli, Environmental performance analysis of textile envelope integrated flexible photovoltaic using life cycle assessment approach, J. Build. Eng. 89 (2024) 109348, https://doi.org/10.1016/j.jobe.2024.109348.